ELSEVIER

Journal of Chromatography A, 911 (2001) 1–12

JOURNAL OF CHROMATOGRAPHY A

www.elsevier.com/locate/chroma

Practical aspects of ultrahigh pressure capillary liquid chromatography

Naijun Wu[a,1], J. Andreas Lippert[b], Milton L. Lee[a,*]

[a]*Department of Chemistry and Biochemistry, Brigham Young University, Provo, UT 84602-5700, USA*
[b]*Department of Chemistry, Weber State University, Ogden, UT 84408-2503, USA*

Received 6 January 2000; received in revised form 15 August 2000; accepted 21 November 2000

Abstract

A novel pressure-balanced injection valve was evaluated for use with ultrahigh pressure liquid chromatography (UHPLC) at pressures up to 120 MPa (1200 bar). Fused-silica capillaries (30–33 cm×100 μm I.D.) packed with nonporous 1.5 μm isohexylsilane-modified (C_6) silica particles were employed to study maximum pressure, injection reproducibility, injection time, and sample amount consumed for an injection. The new valve was more reproducible, convenient, and required much less sample than previously used injection systems. The effect of column diameter on efficiency and sensitivity was studied. The 100 μm I.D. columns demonstrated approximately 40% lower efficiency but 10-fold higher sensitivity than the 29 μm I.D. columns. Columns packed with nonporous C_6 particles produced higher efficiencies than columns packed with a 1.5 μm porous octadecylsilane-modified (C_{18}) material.

Keywords: Capillary columns; Sample introduction; Column packing; Ultrahigh pressure

1. Introduction

In 1975, Halász et al. [1] showed that the fastest separations could be obtained by employing the smallest particles, e.g., particles having diameters of about 1 μm. It was also shown that the minimum analysis time that could be achieved for a given separation was limited by the available inlet column pressure. Most conventional pumping systems have upper pressure limits of ~40 MPa (400 bar), thus confining columns packed with 5 μm particles to lengths of approximately 25 cm and limiting columns employing 1.5 μm particles to a mere 3–4 cm. These columns usually produce 10 000–20 000 plates under typical operating conditions. Recently, MacNair et al. [2,3] introduced ultrahigh pressure capillary liquid chromatography (UHPLC) in order to overcome the pressure limitations that small particles impose on conventional pumping systems. We recently demonstrated both high efficiency and high speed utilizing nonporous C_6-modified silica particles (d_p=1.5 μm) in UHPLC [4]. However, in order to use UHPLC routinely in the laboratory, some practical concerns such as sample introduction, reproducibility, and detection still need improvement.

In UHPLC, sample introduction has been particularly challenging because of the difficulty in

*Corresponding author. Tel.: +1-801-378-2135; fax: +1-801-378-9357.

E-mail address: milton_lee@byu.edu (M.L. Lee).

[1]Present address: Analytical Research Department, Merck Research Laboratories, Rahway, NJ 07065, USA.

0021-9673/01/$ – see front matter
PII: S0021-9673(00)01188-2

constructing a valve that satisfies the sealing requirements at high pressure while concurrently limiting the internal volume to a minimum. Capillary columns used in UHPLC require extremely narrow sample plugs to minimize any sample volume contribution to peak broadening [5]. Conventional commercial injection valves satisfy the requirement for small sample plugs, however, they can only endure pressures of 28–40 MPa (280–400 bar), which are far lower than those required for UHPLC. At this point, all reported UHPLC work has utilized a static-split injection technique that has been described in detail elsewhere [2–4,6]. Using this static-split injection technique, both MacNair et al. [2,3] and this group [4] achieved high column efficiencies because introduced sample plugs were very narrow and symmetric. More importantly, ultrahigh pressures 275–500 MPa (2750–5000 bar) could be applied to these injection systems without leaks. However, several drawbacks of this technique were also evident. First, these sample injection systems require too much sample. Second, the actually injected sample amount cannot be controlled, thus making injections too irreproducible for quantitation. Third, the complete injection process takes several minutes and is inconvenient for practical use. Hence, more reproducible and user-friendly injection systems are desirable.

Another practical consideration for UHPLC is the choice of column, including internal column diameter and packing material. In UHPLC, only capillary columns (e.g., 30–150 μm I.D.) can be used since small column diameters facilitate frictional heat dissipation. Small particles inherently produce very low column permeability and thus, generate considerable heat under high pressure drop and high flow-rate. Poor heat dissipation may result in serious deterioration in column efficiency due to axial and radial temperature gradients [1,2].

Using conventional pumps (e.g., $P<40$ MPa), the effect of column diameter (d_c) on efficiency has been widely investigated in packed capillary LC; it was found that, generally, the performance of the columns improved with decreasing d_c [7–11]. However, some practical problems can arise from reducing d_c. For example, as d_c is reduced, the sensitivity decreases, and the packing process becomes much more challenging. It is still unknown how column diameter affects the performance of UHPLC.

In this study, we evaluated an experimental pressure-balanced injection valve manufactured by Valco (Houston, TX, USA) for use with UHPLC at pressures up to 120 MPa (1200 bar). The pressure limit, injection reproducibility, injection time, and sample amount consumed for an injection were investigated with 100 μm I.D. fused-silica capillary columns (30–33 cm long), packed with nonporous 1.5 μm isohexylsilane-modified (C_6) silica particles; the results were compared with those obtained using previously described static split injection systems. The effect of column diameter on efficiency and sensitivity in UHPLC was studied using 29 and 100 μm I.D. columns. The efficiencies of 29 μm I.D. columns packed with nonporous C_6 particles and a 1.5 μm porous octadecylsilane-modified (C_{18}) material, respectively, were compared.

2. Experimental

2.1. Materials

Acetone, acetonitrile, hexane, and water were HPLC grade and were purchased from Fisher Scientific (Fair Lawn, NJ, USA). Ametryn, atrazine, prometryn, propazine, simetryn, simazine, and terbutryn were obtained from Chem Service (West Chester, PA, USA). Ascorbic acid, catechol, hydroquinone, 4-methylcatechol, and resorcinol were purchased from Sigma (St. Louis, MO, USA). Ammonium acetate and trifluoroacetic acid (TFA) were acquired from Aldrich (Milwaukee, WI, USA). SFC-grade carbon dioxide and compressed nitrogen were obtained from Airgas (Salt Lake City, UT, USA). Fused silica tubing was purchased from Polymicro Technologies (Phoenix, AZ, USA). The nonporous 1.5 μm isohexylsilane-modified (C_6) packing material (Kovasil MS-H) was obtained from Chemie Uetikon (Uetikon, Switzerland). Porous Platinum octadecylsilane-modified (C_{18}) particles (1.5 μm, 80 Å) and cyano-deactivated spherical porous silica (5 μm, 300 Å) particles were purchased from Alltech (Deerfield, IL, USA). Prior to use, all buffers and solvents were filtered through a 0.22 μm Durapore® membrane filter (Millipore, Bedford, MA, USA) and degassed thoroughly. Likewise, samples were degassed and filtered through a 0.2 μm polytetrafluoro-

ethylene (PTFE) syringe filter (Chromacol, Trumbull, CT, USA) before use.

2.2. Column preparation

Fused-silica capillary columns with internal diameters of 29, 75, and 100 μm and an O.D. of 365 μm were packed with nonporous 1.5 μm Kovasil MS-H using a carbon dioxide enhanced slurry packing method [4]. The high-pressure packing system used to prepare the columns for this study was described in a previous paper [4]. Slurries were made in a 33% acetone/67% hexane solution as described by MacMair and coworkers [2]. The slurry (~200 μl) was introduced into the packing reservoir. Liquid carbon dioxide was used as a driving solvent to push the slurry into the column. The initial packing pressure was generally 6 MPa (60 bar). The pressure was raised periodically to maintain a nearly constant packing rate until the column was completely filled. This process was usually completed in less than 30 min. Generally, the final packing pressure ranged between 100 and 140 MPa (1000–1400 bar). The column was then left to depressurize gradually, a process that was routinely completed within 24 h. As reported previously, this method can be used to routinely pack 1.5 μm particles into capillary columns greater than 70 cm in length [4]. Internal column frits to retain the packing material were fabricated using a resistive heating device (InnovaTech, UK) while water was pumped through the column at 80 MPa (800 bar). Once the frits were made, the excess packing material was flushed from the column. The frit maker was also used to remove an approximately 1 mm wide band of the polymeric coating off the fused-silica tubing immediately after the outlet frit of the capillary column to create a window for on-column UV detection.

2.3. Column evaluation

The performances of the columns were assessed with a UHPLC system that is described in detail elsewhere [4]. In short, a double-head air-driven liquid pump (Model DSHF-302, Haskel, Burbank, CA) with a piston area ratio (air drive area to liquid piston area) of 346 was used to generate the necessary liquid pressures. The maximum air supply pressure was 1 MPa (10 bar), resulting in a pump pressure limit of 360 MPa (3600 bar). A cylinder containing compressed nitrogen was used to drive the pump. For this work, the outlet of the pump was connected to either the home-built injection system, the specifics of which have previously been described [4], or to an experimental Valco valve which is described in this paper. Upon injection, data acquisition was initiated.

A mixture containing ascorbic acid (dead-time marker), hydroquinone, resorcinol, catechol, and 4-methylcatechol was used for column testing. The mobile phase consisted of 90% water (containing 0.1% TFA) and 10% acetonitrile. The test mixture was dissolved in mobile phase to a concentration of 20–25 μ*M* per component. A Lee Scientific Model 501 UV/Vis detector was used for on-column monitoring of the UV absorbance of the sample bands as they eluted. Data were acquired with Chrom Perfect 2.2 (Justice Innovations, Mountain View, CA, USA) and processed with a Pentium II 266 MHz computer. Two different data acquisition rates, 10 Hz and 20 Hz, respectively, were used for pressures above and below 140 MPa (1400 bar) to ensure that at least 20 data points were collected to describe each chromatographic peak. The rise time for the UV/Vis detector was 1.0 s. Column efficiencies were calculated from peak widths at half-height and retention times. Digital images of the packing materials were taken using a scanning electron microscope (model JSM-840 A, JEOL, Tokyo, Japan) with a Link ISIS system (Oxford Instruments Limited, Buckinghamshire, UK).

2.4. Valco pressure-balanced injection valve

A new injection valve for evaluation with UHPLC was provided by Valco (Houston, TX, USA). The experimental injector featured a modified 4-port Cheminert Model C2XL flat plate rotary valve. The valve was based on Valco's EXL Technology™ and incorporated a passive feedback system which generated a gradual sealing force on the sample rotor via the mobile phase. In short, the mobile phase exerts pressure on a spring, the tension of which wields a force proportional to the system pressure against the seal. A schematic of this pressure-balanced injection valve is given in Fig. 1. It can be seen that the mobile phase from the pump first passes through the valve body, where its pressure is exerted on a spring-

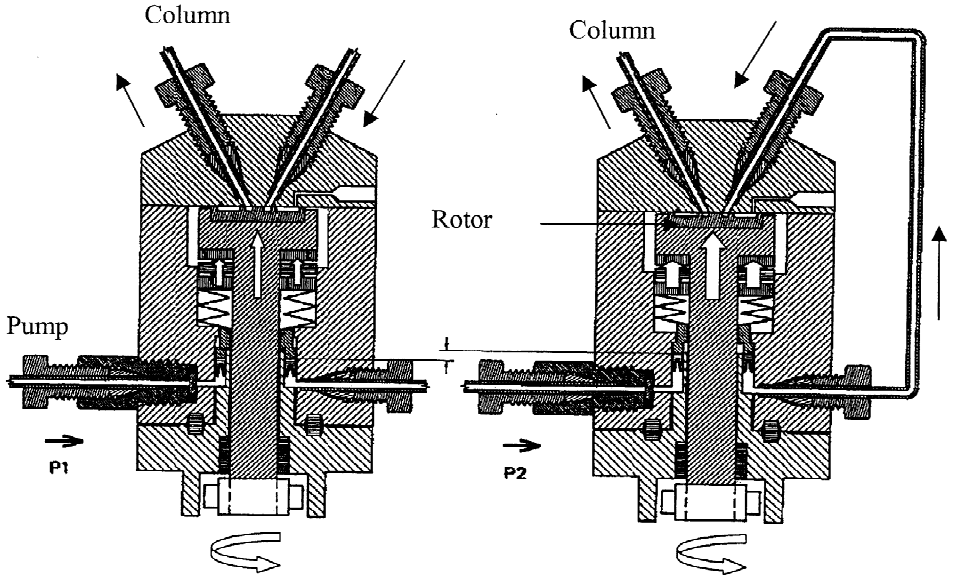

Fig. 1. Schematic of the Valco pressure-balanced injection valve (drawing not to scale). P_1, inlet pressure, where volume begins to expand and spring force starts to rise; P_2, higher inlet pressure, where volume and spring force reach a maximum.

loaded sealing mechanism, before it flows through the stator and the rotor. As the mobile phase pressure is increased from P_1 to P_2, the sealing force transferred from the mobile phase through the springs also increases to maintain the polymeric rotor at nearly isostatic conditions. The valve was equipped with a two-position rotor with 20 nl sample volume. In order to introduce a narrow sample plug into the column, a home-built split injection assembly was used, as shown in Fig. 2. A 5-cm long piece of stainless steel tubing (750 μm I.D., 1.6 mm O.D.) was used to connect a stainless steel tee (750 μm I.D., Valco, Houston, TX, USA) to the injector. A packed capillary column with 365 μm I.D. was slipped through the tee and the metal tubing until it was flush with the end of the latter. The column was then retracted slightly and secured using PEEK tubing (Upchurch, Oak Harbor, WA, USA). The ideal gap between the end of the column and the injector was ~2 mm. If the gap was greater than this, the injected sample was split too much and the detection sensitivity decreased considerably. On the other hand, when the gap was too short, the column efficiency decreased significantly due to the broad sample plug. A piece of fused-silica capillary tubing (2 m×20 μm I.D.) was connected to the third port of the tee to complete the split injection assembly.

3. Results and discussion

3.1. Comparison of pressure-balanced and home-built static split injection valves

3.1.1. Efficiency

In order to achieve maximum performance for a column with small internal diameter, the extra-column band broadening effects must be minimized. The loss in plate number by extra-column broadening effects should not exceed 10% [13,14]. For a specific LC system, the maximum acceptable variance due to extra-column broadening effects can be expressed as [13]:

$$\sigma^2_{e(acc)} \leq 0.10\sigma^2_c \leq 0.10\,\frac{\pi^2 L^2 r^4 \varepsilon^2 (1+k)^2}{N} \qquad (1)$$

where $\sigma^2_{e(acc)}$ is the maximally acceptable variance due to extra-column broadening effects, σ^2_c is the peak variance caused by the chromatographic pro-

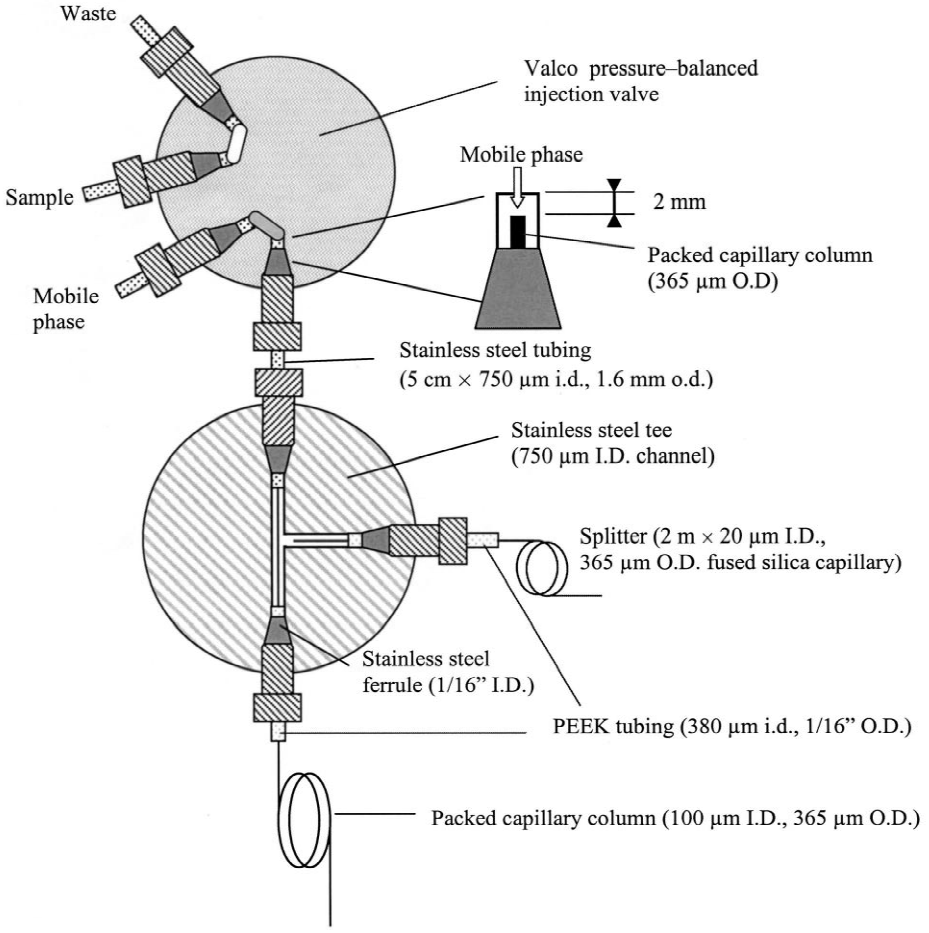

Fig. 2. Schematic of the injector assembly (drawing not to scale).

cess, L is the column length, r is the column radius, ε is the porosity of the column, k is the retention factor, and N is the column efficiency. If extra-column band broadening is mainly caused by the injected sample volume (substantially true for on-column detection), the injection volume variance (V_s^2) is given by [15]:

$$V_s^2 \approx 12\sigma_{e(acc)}^2 \quad (2)$$

From Eqs. (1) and (2), it can be seen that the acceptable injection volume rapidly decreases with decreasing column diameter and column length, and decreases with increasing column efficiency when other parameters are kept constant. Taking $L = 33$ cm, $r = 15$ μm, $k = 0.5$, $\varepsilon = 0.3$ [16] and $N = 100\,000$ as typical conditions for 1.5 μm nonporous particles in UHPLC, the maximum acceptable injection volume can be estimated to be 0.6 nl. When a 100 μm I.D. column is used, this volume is 6.6 nl. For the home-built ultrahigh pressure valve, the injected sample volume for static-split injection was estimated to be 0.2 nl using a 30 cm × 29 μm I.D. column and an injection pressure of 33 bar for 3 s. Due to the narrow sample input width, column efficiencies as high as 300 000–500 000 plates m^{-1} were achieved for 30 μm I.D. columns packed with 1.5 μm particles using this type of injection system [2–4].

However, the minimum injection volume for the

Valco pressure-balanced valve was 20 nl, which is still too large for typical UHPLC columns. Initially, we tried to directly inject the sample into a column, however, the measured efficiency was lower than 100 000 plates m^{-1}, which is much lower than expected (300 000 plates m^{-1}). When the split injection assembly was used, the column efficiency improved greatly. Fig. 2 illustrates how the home-built injection assembly is used to split the injected sample. When a sample plug moves from the Valco injector into the 750 μm I.D. stainless steel tubing, the plug width decreases significantly because the inner diameter of the stainless steel tubing is much larger than that of the sample plug. Hence, a much narrower sample plug is introduced at the column inlet. Most of the sample is flushed out through the splitter. The split ratio is approximately 1:220. It should be noted that the split ratio used in this study was much higher than calculated (6.6 nl/20 nl = 1:3). This may be explained by the fact that when the sample plug moved from the injector rotor into the stainless steel tubing, some turbulence occurred which deformed the sample plug. This deformation became less significant when high split ratios were used. However, if the split ratio was too high, the ultrahigh pressure pump, which has a stroke volume of 4.5 ml, recycled often, thus causing irregularities in the baseline and shortening the lifetime of the columns by forming gaps in the packed bed. Theoretically, if the connection between the injection valve and capillary column is perfect, the extra-column band broadening from injection will decrease significantly. For static split injection, the sample plugs were not only narrow but also very symmetric because the column inlet was inserted into a large channel (1.5 mm I.D.) which was full of the sample solution.

An average column efficiency as high as 300 000 plate m^{-1} was obtained using a 33 cm × 100 μm I.D. column packed with nonporous 1.5 μm Kovasil particles using the experimental Valco valve and a test mixture containing ascorbic acid, hydroquinone, resorcinol, catechol, and 4-methylcatechol. This is comparable to efficiencies obtained using the home-built static-split injection valve. Fig. 3A shows a separation of a herbicide mixture using the pressure-balanced injection valve and a 30 cm × 100 μm I.D. capillary column packed with 1.5 μm Kovasil MS-H

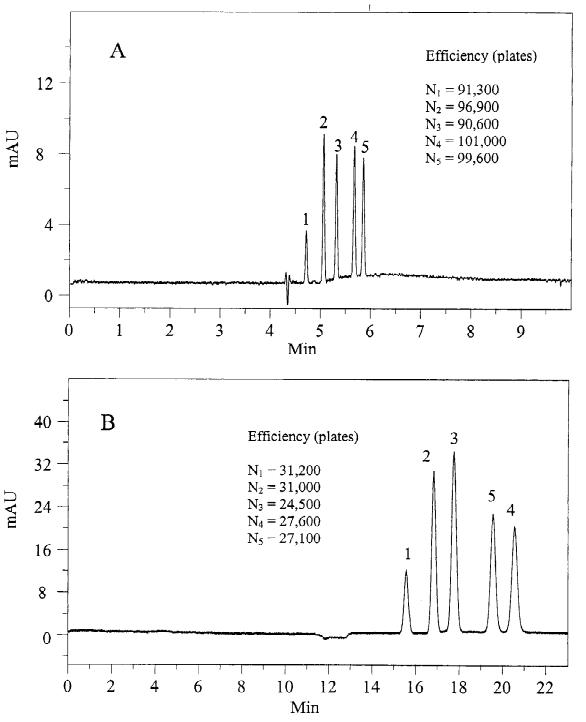

Fig. 3. Chromatograms of a herbicide mixture. Conditions: (A) 30 cm × 100 μm I.D. fused-silica capillary column packed with nonporous 1.5 μm Kovasil MS-H particles; 100 MPa (1000 bar); 20 nl Valco pressure-balanced injection valve; room temperature; 20 m*M* ammonium acetate (pH 3.5)/acetonitrile (60:40,v/v); 215 nm UV detection. (B) 30 cm × 100 μm I.D. fused-silica capillary column packed with porous 5 μm cyano-bonded particles; 3.5 MPa (35 bar). Other conditions are the same as in (A). Peak identifications: (1) simazine, (2) ametryn, (3) prometryn, (4) terbutryn, (5) propazine.

nonporous particles. It can be seen that the separation was accomplished in 6 min with an average total column efficiency of 96 000 plates (320 000 plates m^{-1}) at 100 MPa (1000 bar) inlet pressure. When a column of identical dimensions, packed with porous 5 μm particles was used, the separation required 21 min, which is 3.5 times slower than in UHPLC using 1.5 μm nonporous particles, as shown in Fig. 3B. The average efficiency for the latter separation was 28 100 plates, which is approximately 3.4 times less than that obtained in UHPLC. It should be noted that the pressure required for the column packed with 5 μm porous particles was only 3.5 MPa (35 bar), which is 30 times lower than what was required for the column packed with 1.5 μm

nonporous material. As predicted by theory, the pressure required to achieve the optimum flow-rate is inversely proportional to the cube of the particle diameter [2]. Since both separations were made near the respective optimum linear velocities (u_{opt}), the pressure required for 5 μm particles should be 37 times lower than that for 1.5 μm particles, assuming that retention factors and diffusion coefficients are the same. However, the pressure (3.5 MPa) used for 5 μm porous particles in this study was somewhat higher than expected (2.8 MPa). This may be explained by the fact that porous particles produce a higher pressure drop than nonporous particles [17,18].

3.1.2. Reproducibility

Table 1 compares the reproducibilities of the two injection modes. It can be seen that there are no significant differences in reproducibilities of column efficiency and retention time for the two injection systems. However, the relative standard deviation (RSD) of peak area for the Valco pressure-balanced system is much lower compared to the home-built static-split injection system. For the pressure-balanced valve injector, the injected sample amount mainly depends on the time interval of switching and the split ratio. These two factors are usually easy to control. For the static-split injector, the injected sample amount is affected by injection pressure, time interval of valve opening and closing, depressurization time of the column, and sample flushing. According to our experience, the second factor was the most difficult to control. The operation of this valve required two complete revolutions of the valve handle, i.e., it usually took 3–4 s to open and close this valve. The actual injection time may change in a greater range from run to run. In addition, the remaining pressure in the column also affects the injected sample amount. Thus, it is important to keep the depressurization time constant. The reproducibility of injected sample amount is a critical factor for quantitative analysis, especially when an external standard method is used. For this reason, the Valco pressure-balanced valve is more suitable for routine laboratory use.

3.1.3. Other injection parameters

Other practical injection parameters for the two injection systems are compared in Table 2. It can be seen that the time required for injection is 1–3 min for the home-built static-split injection system, which is mainly due to the time required for depressurization and sample flushing. This time is almost comparable to the separation times for simple separations. Depressurization is necessary because static-split injection is carried out under near zero pressure drop. However, depressurization cannot be too fast; otherwise, gaps are easily formed at the column inlet. In contrast, injection using the Valco pressure-balanced valve was made under constant pressure. Thus, injection was very convenient and it only required 2–3 s. The static-split injection system also required a large volume of sample, e.g., 80–120 μl, although the actual sample injected into the column was much lower. This would prohibit many separations for which only small samples are available. In addition, the mobile phase consumed for every 100 runs would be high (650–700 ml) for the static-split injection system.

It can be seen from Table 2 that ultrahigh pressures (e.g., 360 MPa) can be applied to the home-built injection system without leaking. With

Table 1
Reproducibilities of pressure-balanced and static-split injection valves[a]

	Pressure-balanced valve		Static-split valve	
	Average[b]	RSD (%)	Average[b]	RSD (%)
Column efficiency (plates)	102 000±1400	1.4	105 000±1600	1.5
Retention time (min)	7.32±0.04	0.53	7.41±0.06	0.81
Peak area (mV×s)	98 400±1600	1.7	130 600±26 700	20.4

[a] Conditions: 33 cm×100 μm I.D. fused-silica capillary column packed with 1.5 μm Kovasil MS-H nonporous particles; two columns were tested and 5 measurements for each column were made; hydroquinone (2.5 mg ml^{-1}) test solute ($k=0.07$); 100 MPa (1000 bar) inlet pressure; room temperature; water (0.12% TFA)/acetonitrile (90:10 v/v), 215 nm UV detection.

[b] Confidence intervals were calculated at 95% confidence level.

Table 2
Comparison of various injection parameters for valve injectors[a]

	Pressure-balanced valve	Static-split valve
Total injection time	1–2 s	1–3 min, including depressurization, flushing, and injection
Sample amount injected	2–3 μl	100–150 μl
Mobile phase consumed/100 runs	<10 ml	650–700 ml
Maximum pressure (MPa)	120	360
Maximum plates/column	100 000–200 000[b]	300 000–450 000[c]

[a] Conditions: 100 μm I.D. fused-silica capillary column packed with 1.5 μm Kovasil MS-H nonporous particles; 100 MPa (1000 bar) inlet pressure; room temperature; water (0.1% TFA)/acetonitrile (90:10 v/v), 215 nm UV detection.
[b] 30–33 cm capillary columns packed with uniform nonporous 1.5 μm particles, 100 MPa (1000 bar) pressure.
[c] 90–100 cm capillary columns packed with the same particles as in b, 310 MPa (3100 bar) pressure.

this system, a column as long as 90 cm packed with nonporous 1.5 μm particles can be used to generate total column efficiencies as high as 300 000–450 000 plates at u_{opt}. However, the maximum pressure the Valco pressure-balanced system could tolerate without leakage was 120 MPa (1200 bar). Therefore, the highest continuous pressure employed with this valve was 100 MPa (1000 bar); this resulted in a maximum average total column efficiency of 100 000 plates when a 33 cm long column packed with 1.5 μm nonporous particles was used (see Table 2).

3.2. Column considerations

3.2.1. Effect of column diameter on efficiency

The effect of column diameter on column efficiency was investigated at pressures ranging from 35 to 275 MPa (350–2750 bar) using 29 and 100 μm I.D. columns packed with nonporous 1.5 μm particles. Table 3 summarizes the performance of the different columns studied. It can be seen that column efficiency decreased as the column diameter increased. On average, theoretical plate numbers for the 29 μm I.D. columns were approximately 36% higher compared to the 100 μm I.D. columns. The van Deemter plots for 29 and 100 μm I.D. columns are shown in Fig. 4. The curve for the 29 μm I.D. columns is more flat in the right half of the plot and has a lower reduced plate height minimum than the curve representing the 100 μm I.D. columns. This means that in comparison to the 100 μm I.D. columns, the 29 μm I.D. columns had smaller eddy diffusion (A term) and mass transfer resistance (C term) contributions to band broadening. Smaller eddy diffusion could be interpreted as a narrowing of the flow-rate distribution over the column cross-section as the column diameter decreases. Coupled to this is the shorter time needed for the solute molecules to radially diffuse through the entire flow velocity

Table 3
Experimentally determined column efficiencies and reduced plate heights for columns with internal diameters of 29 and 100 μm[a]

Column I.D. (μm)	N_{max} (plates m^{-1})	h_{min}
29	490 000, 444 000	1.4, 1.5
100	293 000, 303 000	2.3, 2.2

[a] Conditions: 33 cm fused-silica capillary columns packed with 1.5 μm Kovasil MS-H nonporous particles; two columns were tested for each internal diameter, hydroquinone (2.5 mg ml^{-1}) test solute; room temperature; water (0.1% TFA)/acetonitrile (90:10 v/v), 215 nm UV detection.

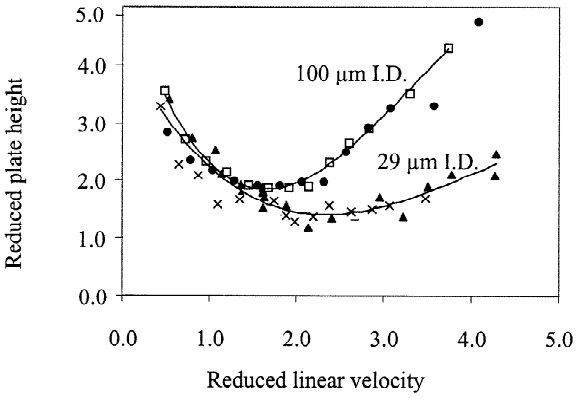

Fig. 4. van Deemter plots for 29 and 100 μm I.D. columns. Conditions are the same as in Table 3. Two columns (shown by different symbols) were tested for each internal diameter columns and the averages were used to plot the curves; D_m value of 7.7×10^{-6} cm^2 s^{-1} for hydroquinone [7].

profile, relaxing the effect of flow anisotropy [19]. In addition, a decrease in retention inhomogeneities with column diameter may contribute to a decrease in the eddy diffusion term [7].

Lower resistance to mass transfer for a small I.D. column could be explained by the wall-effect. This effect has been widely used to interpret the fact that a packed column with an aspect ratio (ratio of column diameter to particle diameter) lower than 6 produces a lower reduced plate height than a column with an aspect ratio higher than 8 [20,21]. In this study, the aspect ratios for columns ranged from 19 to 67, which is much higher than 8. However, we found that the average retention factors obtained from columns with 100 μm I.D. packed with 1.5 μm particles were 10–15% higher compared to 29 μm I.D. columns. This implies that the packing in the 100 μm I.D. columns was more dense than in the 29 μm I.D. columns. Therefore, it is more likely that the particle density gradient across the column for the wall effect is more gradual than suggested by Knox and Parcher [20]. Baur et al. [22] investigated the radial dispersion from conventional HPLC columns and found that the plate height became constant over 25–30 particle diameters from the edge of the column. Witowski and Kennedy [11] recently showed that significant wall-effect occurred even when the aspect ratio was greater than 11. In Fig. 4, no obvious difference in the slopes of the left-half plots was observed between 29 and 100 μm I.D. columns, This suggests that there should be no trend in dependence of longitudinal diffusion (B term) on internal column diameter in UHPLC. More theoretical and experimental work is needed to thoroughly investigate the mechanism of the effect of the column internal diameter on efficiency under ultra-high pressures.

3.2.2. Effect of column diameter on detection and injection

Although sensitive electrochemical detectors have been used in UHPLC [2,3], UV detectors are more universal and robust. In this work, an on-column window was made and a UV detector was used. Fig. 5 shows the peak intensities of three chromatograms obtained using 29, 75, and 100 μm I.D. columns. It can be seen that the peak intensity decreases significantly with decreasing column diameter. The

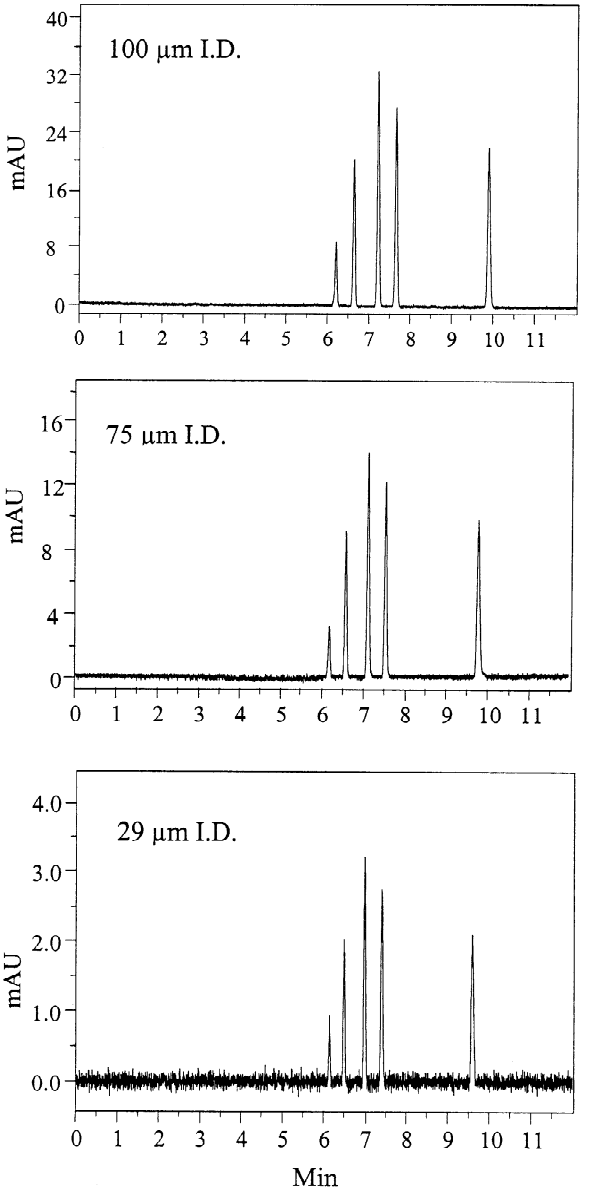

Fig. 5. Chromatograms of a standard mixture using columns with different internal diameters. Conditions: 33 cm fused-silica capillary columns packed with 1.5 μm Kovasil MS-H nonporous particles; 15 Kpsi inlet pressure; room temperature; water (0.1% TFA)/acetonitrile (90:10 v/v), 20 nl Valco pressure-balanced injection valve; 215 nm UV detection. Peak identifications (from left to right): ascorbic acid, hydroquinone, resorcinol, catechol and 4-methylcatechol.

peak height for a 100 μm I.D. column is 10 times higher than that for a 29 μm I.D. column. This implies that 100 μm I.D. columns can give 10-fold higher sensitivity than 29 μm I.D. columns. This value, however, is higher than that predicted by the Beer–Lambert law due to an increase in spatial stray light for small I.D. columns [10].

Another practical consideration is the effect of column internal diameter on sample capacity. Theoretically, sample capacity increases proportionally with the square of column diameter [23]. Thus, the sample capacity for a 100 μm I.D. column is ~12 times that for a 29 μm I.D. column. Combining the two advantages in sensitivity and sample capacity, the sample linear dynamic range for a 100 μm I.D. column can be 10–100 times greater than that for a 29 μm I.D. column. Therefore, there are tradeoffs between column efficiency, sensitivity, and sample capacity.

3.2.3. Effect of column packing on performance

Recently, Knox emphasized that better packing of HPLC columns can certainly produce much more efficient columns [24]. Better packing means that more uniform particles and better packing methods should be used. The high efficiencies obtained from 1.5 μm Kovasil MS-H nonporous particles in this study can be attributed to the exceptional uniformity of the particles used. Fig. 6 shows scanning electron micrographs of uniform and nonuniform 1.5 μm particles in capillary columns. The particle size distribution and shape were verified using image processing tool plug-in software for Adobe Photoshop 5.0. The % RSD of the diameters of the nonporous particles was 3.8% ($n=160$) compared to 35.4% ($n=77$) for porous particles. Furthermore, the carbon dioxide-slurry packing method can produce uniformly packed columns [12]. As shown in Fig. 6A, a very tight and uniform packing pattern can be seen for 1.5 μm Kovasil nonporous particles. The small particles used in this work exhibited a tendency to agglomerate, allowing only the packing of several centimeters in initial attempts. This problem was overcome by forming a silica particle slurry with an organic solvent, and subsequently driving the slurry through the column with liquid carbon dioxide. Liquid carbon dioxide has a lower viscosity than most organic solvents, which facilitates pumping the particles into the capillary and forming a uniform bed.

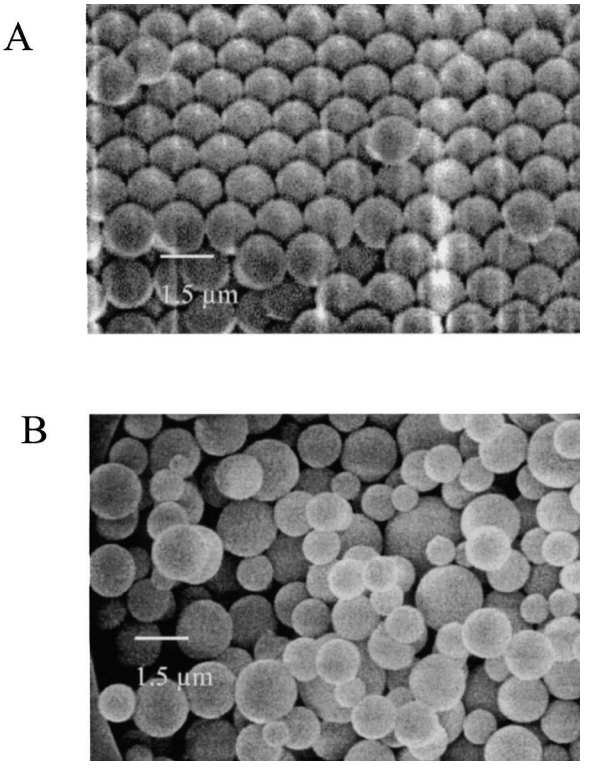

Fig. 6. Scanning electron micrographs (magnification = ×9000) of 1.5 μm (A) uniform and (B) nonuniform particles in capillary columns.

Until now, only nonporous particles have been used in UHPLC. The reason for this is that columns containing nonporous silica (NPS) particles always exhibit better efficiencies than porous silica (PS) particles for particles of the same dimension. Table 4 lists the column efficiencies for PS and NPS particles. It can be seen that the average theoretical plate number for a 33 cm×29 μm I.D. column packed with 1.5 μm Kovasil MS-H NPS particles is ~3 times higher compared to 1.5 μm Alltech ODS PS particles under near optimum conditions (similar *k* values and separation times). As illustrated in Fig. 6B, 1.5 μm Alltech porous ODS particles have a very poor size distribution. This can result in a large eddy diffusion term, and thus, low column efficiency. In addition, the poor size distribution can cause loose packing and high mass transfer resist-

Table 4
Efficiencies (plates m^{-1}) for columns containing porous and nonporous particles[a]

Particles	Ascorbic acid	Hydroquinone	Resorcinol	Catechol	4-methyl-catechol	Average
	449 000	432 000	429 000	430 000	442 000 (0.50)[b]	
Nonporous						423 000
	438 000	402 000	393 000	394 000	421 000 (0.55)	
	109 000	138 000	143 000	147 000	144 000 (0.49)	
Porous						140 000
	112 000	147 000	145 000	158 000	152 000 (0.50)	

[a] Conditions: 33 cm×29 μm I.D. fused-silica capillary columns (two columns tested), 215 nm UV detection. For nonporous particles: 1.5 μm Kovasil MS-H; water (0.1% TFA)/acetonitrile (90:10 v/v), 155 MPa (1550 bar) inlet pressure. For porous particles: 1.5 μm, 80 Å, Alltech Platinum C_{18} PS particles; water (0.1% TFA)/acetonitrile (50:50 v/v); 100 MPa (1000 bar) inlet pressure.
[b] Values in parentheses are retention factors of 4-methylcatechol.

ance, which can also contribute to low efficiency. Finally, the mass transfer resistance in the stagnant mobile phase in pores for porous particles increased the total mass transfer resistance, which further decreased column efficiency. The mass transfer resistance in the stagnant mobile phase for 1.5 μm Alltech ODS PS particles is approximately four times higher than the total mass transfer resistance for 1.5 μm Kovasil MS-H NPS particles [25]. Therefore, the NPS particles gave a much flatter van Deemter profile and could therefore be operated at much higher linear velocity without considerable loss in efficiency. Thus, NPS particles have a distinct advantage for fast separations. However, columns containing PS particles provide higher sample capacity. A 77 cm×50 μm I.D. column packed with PS particles of 3 μm could provide about four times the sample capacity of 3 μm NPS particles [25].

4. Conclusions

The pressure-balanced injection system evaluated in this study is more reproducible, convenient, and requires much less sample volume and mobile phase than the static-split injection system. This injection system permitted routine operation at pressures up to 100 MPa (1000 bar). The column internal diameter has a considerable effect on column efficiency, sensitivity, and sample capacity. While 29 μm I.D. columns generated almost 40% more plates than 100 μm I.D. columns at the optimum linear velocities, 100 μm I.D. columns provided 10 times higher sensitivities and sample capacities compared to 29 μm I.D. columns when on-column UV detection was used. Typically, 30 cm×100 μm I.D. columns packed with nonporous 1.5 μm particles produced about 3.5 more plates in less than one-third of the time required to complete a separation with a column packed with porous 5 μm particles. Hence, 100 μm I.D. capillary columns packed with nonporous 1.5 μm particles seem more practical for quantitative analysis in UHPLC. Finally, while the pressure-balanced injection system is a step forward in the development of UHPLC for routine analysis work, an injector that can withstand even higher pressures, e.g. 200–400 MPa (2000–4000 bar), is still desirable.

Acknowledgements

This work was partially funded through a grant from G.D. Searle, Research and Development Division, Skokie, IL, to Brigham Young University (BYU). The authors thank Stan Stearns from Valco Instruments for providing the experimental injection valve used in this work, and for valuable discussions related to high-pressure sample introduction in capillary LC.

References

[1] I. Halász, R. Endele, J. Asshauer, J. Chromatogr. 12 (1975) 37.
[2] J.E. MacNair, K.C. Lewis, J.W. Jorgenson, Anal. Chem. 69 (1997) 983.

[3] J.E. MacNair, K.D. Patel, J.W. Jorgenson, Anal. Chem. 71 (1999) 700.
[4] J.A. Lippert, B. Xin, N. Wu, M.L. Lee, J. Microcol. Sep. 11 (1999) 631.
[5] J.P.C. Vissers, H.A. Claessens, C.A. Cramers, J. Chromatogr. A 779 (1997) 1.
[6] J.W. Jorgenson, E.J. Guthrie, J. Chromatogr. 255 (1983) 335.
[7] K.E. Karlsson, M. Novotny, Anal. Chem. 60 (1988) 1662.
[8] R.T. Kennedy, J.W. Jorgenson, Anal. Chem. 61 (1989) 1128.
[9] L.J. Cole, N.M. Schultz, R.T. Kennedy, J. Microcol. Sep. 5 (1993) 433.
[10] S. Hsieh, J.W. Jorgenson, Anal. Chem. 68 (1996) 1212.
[11] S.R. Witowski, R.T. Kennedy, J. Microcol. Sep. 11 (1999) 723.
[12] A. Malik, W. Li, M.L. Lee, J. Microcol. Sep. 5 (1993) 361.
[13] E.S. Yeung, in: M.V. Novotny, D. Ishii (Eds.), Microcolumn Separations, Elsevier, Amsterdam, 1985, p. 117, Journal of Chromatography Library, Vol. 30.
[14] J.C. Gluckman, in: M.V. Novotny, D. Ishli (Eds.), Microcolumn Separations, Elsevier, Amsterdam, 1985, p. 57, Journal of Chromatography Library, Vol. 30.
[15] M. Krejčí, in: Trace Analysis With Microcolumn Liquid Chromatography, Marcel Dekker, New York, 1992, p. 35.
[16] H. Giesche, K.K. Unger, U. Esser, B. Eray, U. Trildinger, J.N. Kinkel, J. Chromatogr. 465 (1989) 39.
[17] Y. Shen, Y.J. Yang, M.L. Lee, Anal. Chem. 69 (1997) 628.
[18] N. Wu, Q. Tang, Y. Shen, Anal. Chem. 71 (1999) 5084.
[19] P.A. Bristow, J.H. Knox, Chromatographia 10 (1977) 279.
[20] J.H. Knox, J.F. Parcher, Anal. Chem. 41 (1964) 1599.
[21] J.C. Sternberg, R.E. Poulson, Anal. Chem. 6 (1964) 1492.
[22] J.E. Baur, E.W. Kristensen, R.M. Wightman, Anal. Chem. 60 (1988) 2334.
[23] G. Guiochon, in: P. Kucera (Ed.), Microcolumn High-performance Liquid Chromatography, Kucera, Amsterdam, 1984.
[24] J.H. Knox, J. Chromatogr. A 831 (1999) 3.
[25] J.A. Lippert, N. Wu, M.L. Lee, presented at the 22nd International Symposium on Capillary Chromatography, Gifu, Japan, Nov. 8–12, 1999.